Organic & Biomolecular Chemistry

COMMUNICATION

View Article Online
View Journal | View Issue

Cite this: *Org. Biomol. Chem.*, 2017, **15**, 6710

Received 30th June 2017,
Accepted 25th July 2017

DOI: 10.1039/c7ob01592e

rsc.li/obc

Facile functionalization of peptide nucleic acids (PNAs) for antisense and single nucleotide polymorphism detection†

Digvijay Gahtory, [a] Merita Murtola,[b] Maarten M. J. Smulders, [a] Tom Wennekes, [a,c] Han Zuilhof, *[a,d,e] Roger Strömberg *[b] and Bauke Albada *[a]

In this report, we show how a convenient on-resin copper-click functionalization of azido-functionalized peptide nucleic acids (PNAs) allows various PNA-based detection strategies. Firstly, a thiazole orange (TO) clicked PNA probe facilitates a binary readout when combined with F/Q labeled DNA, giving increased sensitivity for antisense detection. Secondly, our TO-PNA conjugate also allows single nucleotide polymorphism detection. Since antisense detection is also possible in the absence of the TO label, our sensing platform based on azido-D-ornithine containing PNA even allows for additional and more advanced functionalization and sensing strategies.

Since the discovery of peptide nucleic acids (PNAs),[1] they have been employed for numerous applications in molecular biology,[2] antisense technology,[3] and nucleic acid detection.[4] Generally, the PNA structure is composed of a polyamide backbone consisting of *N*-(2-aminoethyl)glycine (Aeg)[5] or other amino acid units,[6] with the nucleobases linked *via* an amide linkage. This biomimetic structure makes them compatible with biology, yet renders them resilient to enzyme-catalyzed degradation.[7] Furthermore, DNA–PNA duplexes have higher melting points than similar DNA–RNA or DNA–DNA duplexes.[8] The biomimetic properties of PNA have led to a growing interest in their utilization as carriers for the delivery of antisense DNA/RNA molecules for inhibition of gene expression, for example using cell penetrating peptide (CPP)–PNA conjugates.[9] PNA has even been used as a basis for artificial RNases.[10]

Seitz *et al.* reported that replacing one of the nucleobases with an intercalating fluorophore provides so-called *forced intercalation* probes that possess an excellent single nucleotide polymorphism (SNP) detection ability.[11] Specifically, it was shown that replacement of a PNA backbone unit to which thiazole orange (TO) is anchored from Aeg to D-ornithine (^{D}Orn) increased the SNP detection ability.[12,13] In this approach, TO is still linked to the PNA backbone *via* an amide-group (Fig. 1a and b). Although click chemistry has been widely applied in the past decade,[13] *e.g.* on incorporated azido-functionalized nucleobases[14] or *via* a flexible azido/alkyne tether,[15] this chemistry was not yet applied to attach forced intercalation probes to a PNA backbone. In this study, we assess the extent to which the triazole linkage is also a good isostere for amide bonds in this setting,[16] specifically related to two sensing applications for TO-functionalized PNA.

Here, we report a click strategy for resin-bound PNA using α-azido D-ornithine, that can be incorporated in the PNA chain during standard Fmoc-based solid-phase PNA synthesis. Once incorporated, the azido group allows direct attachment of thiazole orange (TO), illustrating its convenience as handle for PNA diversification. We used an on-resin copper-catalyzed azide–alkyne click (CuAAC) reaction to attach the dye to the

[a]*Laboratory of Organic Chemistry, Wageningen University and Research, Stippeneng 4, 6708 WE Wageningen, The Netherlands. E-mail: han.zuilhof@wur.nl, bauke.albada@wur.nl*
[b]*Department of Biosciences and Nutrition, Novum, Hälsovägen 7, 141 83 Huddinge, Sweden. E-mail: roger.stromberg@ki.se*
[c]*Department of Chemical Biology and Drug Discovery, Utrecht Institute for Pharmaceutical Sciences and Bijvoet Center for Biomolecular Research, Utrecht University, Utrecht, The Netherlands*
[d]*Department of Chemical and Materials Engineering, King Abdulaziz University, Jeddah, Saudi Arabia*
[e]*School of Pharmaceutical Sciences and Technology, Tianjin University, 92 Weijin Road, Tianjin 300072, P.R. China*

†Electronic supplementary information (ESI) available: Synthesis of alkyne-derivatized thiazole orange **1**, additional ^{1}H NMR spectra, ESI-MS, HPLC traces and fluorescence data. See DOI: 10.1039/c7ob01592e

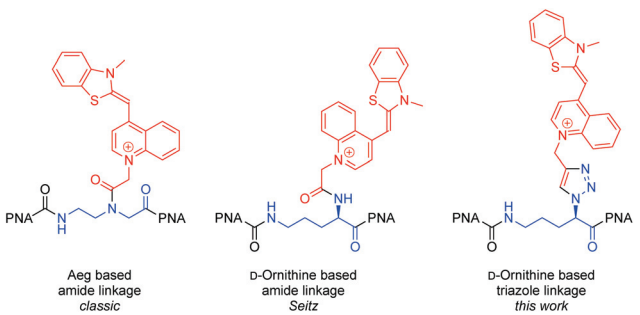

Fig. 1 Structural comparison of a thiazole orange (red structure) fluorophore linked to PNA by an amide on Aeg (left) and ^{D}Orn (middle), respectively, *versus* triazole linkage (right).

resin-bound PNA chain. The resulting TO-PNA construct was then tested as a sensing module in (i) FRET-assisted antisense detection, and (ii) single nucleotide mismatch detection. For comparison, the azido-PNA precursor was tested in regular antisense detection.

First, we prepared a DNA binding motif based on PNA. As shown by Seitz *et al.*, a D-ornithine linker successfully mimics the six-atom long building block that normally forms the PNA backbone, facilitating optimal PNA nucleobase alignment for hybridization with DNA or RNA.[11] Accordingly, resin-bound PNA that contained azido-D-ornithine (**P1**) was prepared using standard procedures (Scheme 1 and see ESI, Fig. S1–S3† for crude HPLC traces of **P1**). C- and N-terminal lysine residues were incorporated in the longer PNA sequences **P1** and **P3** in order to increase the solubility of the PNA sequence; the azido-D-ornithine residue was sandwiched in between two adenine bases to achieve a low fluorescence F_0 in the single stranded form after functionalization with TO.[11b] Following this, resin-bound PNA underwent a facile CuAAC with alkyne-derivatized thiazole orange **1** (see ESI† for synthesis; λ_{ex} = 510 nm, λ_{em} = 530 nm), to yield resin-bound TO-PNA conjugate **P2**. After acidic removal of TO labeled PNA **P2** from the resin, TO-PNA conjugates **P3** and **P4** were obtained in good yields (40% after HPLC purification) (Scheme 1 and see ESI, Fig. S4–S6† for HPLC traces and absorbance spectrum of conjugate **P3**).

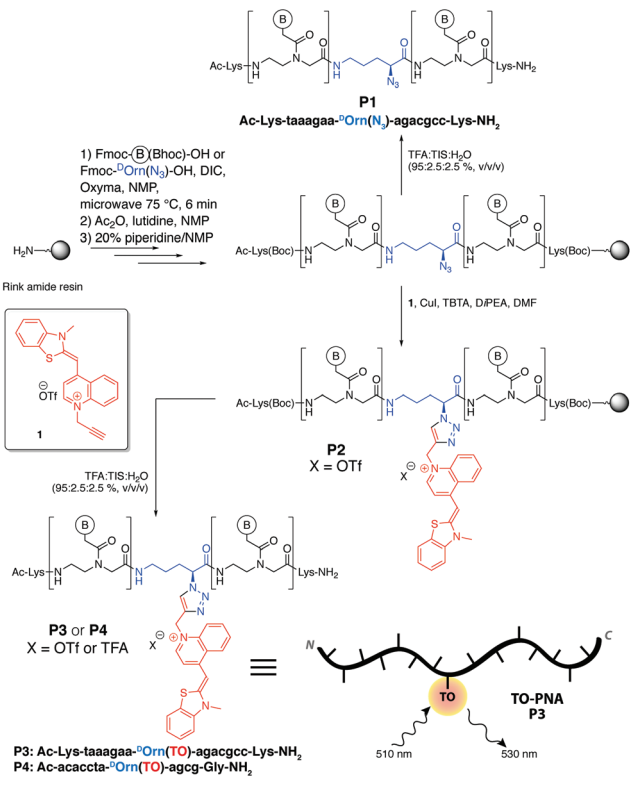

Scheme 1 General scheme for synthesis of DOrn-containing PNA (**P1**) and on-resin click with thiazole orange (TO) to give clicked PNA (**P2**), which after acidic cleavage and deprotection yields soluble TO-PNA **P3**; a similar procedure leads to SNP-sensor **P4**.

For DNA detection, we pursued partial hybridization of the PNA strand to a sequence **D1** that was labelled with a fluorophore–quencher pair of Cy5 (F) (λ_{ex} = 650 nm, λ_{em} = 668 nm) and black hole quencher Iowa Black (Q) (λ_{max} = 667 nm), at the 5′- and 3′-ends of the oligonucleotide chain, respectively. The oligonucleotide sequence was chosen so that it would form a circular DNA–PNA heterodimer in which the labeled termini of the DNA bind to the middle section of the PNA sequence, close to the TO moiety (see Scheme 2a); an internal stretch of ssDNA would provide the sensing sequence located at the opposite side of the circle with respect to the TO label. Specifically, the overall design provides significant binding to two 7 bp-long termini of **P1** while providing a ssDNA docking site of 7 bp for an incoming oligonucleotide that would be complementary to **D1**. In this configuration, the fluorophore and black hole quencher are in close proximity to each other and to the TO dye. As a result, the FRET from TO to Cy5 is quenched by the Iowa Black quencher. In the presence of a DNA trigger, however, the F/Q-labelled DNA strand should be released from the DNA–PNA heterodimer *via* a competitive hybridization stimulus, resulting in the formation of dsDNA and a concomitant separation of Cy5 from the TO label and from the Iowa Black quencher, leading to an increase in the fluorescent signals emanating from both **D1** and **P3**. As an alternative to the direct antisense detection, the presence of a TO-moiety in the middle of a PNA strand would also facilitate direct detection of single nucleotide polymorphisms (Scheme 2b). Alternative to the application of the azido moiety for conjugation to a dye that allows advanced sensing approaches, the azido group could also function as a handle for further functionalization, *e.g.* with a bioactive moiety.

The sensing ability of the DNA–PNA duplex was tested using an antisense sequence that binds to the normal luciferase mRNA, *i.e.* 5′-TTCTTTATGTTTTTGGCGTCT-3′; this sequence was chosen to be applied in CPP–PNA delivery vectors.[9a] Initially, we tested the sensing ability of the azido-functionalized PNA **P1** in combination with F/Q-functionalized DNA **D1**. Mixing **D1** and **P1** indeed resulted in a 6-fold decrease in fluorescence intensity at 667 nm when compared to **D1** alone (Fig. S7†). Upon addition of **D2**, which is fully complementary to **D1**, a 2-fold increase in fluorescence was observed at λ_{em} = 667 nm when compared to **D1** alone, along with a shift of λ_{em} to a higher wavelength (λ = 695 nm). Interestingly, at 695 nm the difference in intensities was significantly higher, *i.e.* 25-fold. Comparing the intensity of the **D1–P1** duplex at 667 nm with that of the **D1–D2** duplex at 695 nm displays a 10-fold increase in fluorescence as result of the sensing event. For further discussions regarding the sensing ability of the azido-functionalized PNA **P1**, see ESI (Fig. S7† and accompanying discussion).

In addition to this antisense detection approach, we observed a difference of 10 °C in T_M value (ΔT_M) between the two complexes (see ESI, Fig. S8†), *i.e.* **D1–P1** and **D1–D2**. The higher T_M for **D1–D2** when compared to **D1–P1** shows that the former duplex was more tightly associated than the latter hybrid duplex. Although PNA–DNA duplexes usually have a

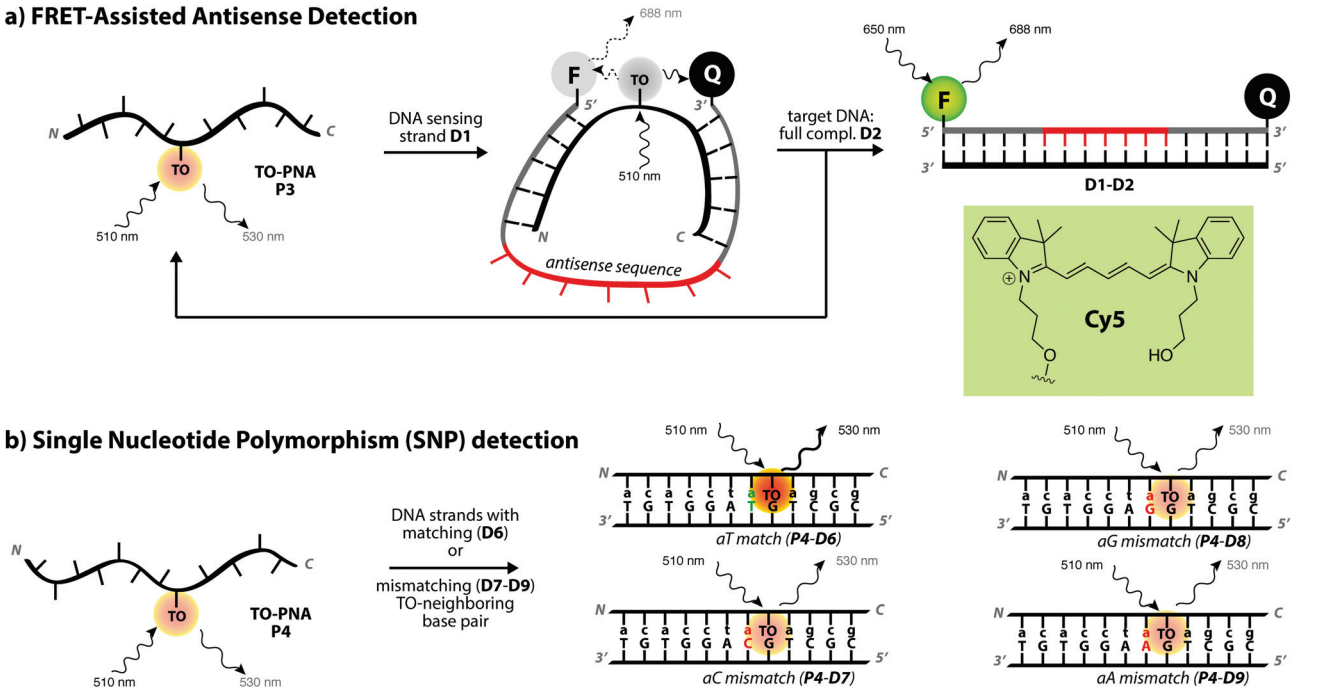

Scheme 2 Overview of the sensing approaches that are described in this study. The wavy arrows indicate the irradiation or emission events of a fluorophore (F or TO), the dotted wavy arrow (in panel a) indicates low intensity emission due to quenching by a nearby organic black hole quencher (Q, panel a). (a) Schematic depiction of the FRET-assisted antisense detection system based on TO-labelled PNA **P3**. Hybridization with F and Q labelled DNA sensor strand **D1**, the dyes Cy5 and TO are in close proximity of the quencher, leading to reduced fluorescence of TO, which results in poor FRET and concomitant lower emission from Cy5. Fluorescence of both TO and Cy5 is restored after replacement of the PNA **P3** with a fully complementary target strand **D2**. (b) Schematic representation of hybridization between TO-PNA (**P3**) and matched/mismatched DNA, showing the single nucleotide polymorphism (SNP) detection approach in which the TO label senses the match/mismatch pair of its neighboring base.

higher T_M than DNA–DNA duplexes that have the same sequences, the lower T_M of the **D1–P1** duplex can be explained by the presence of 7 additional base pairs in **D1–D2** when compared to **D1–P1**.

Realizing that it would be beneficial to be able to directly monitor the association and dissociation of labeled DNA to the PNA, we attached TO (**1**) to the resin-bound PNA (**P2**), resulting in TO-PNA (**P3**), allowing us to measure FRET between TO and Cy5 (Scheme 2a). Indeed, although the fluorescence intensity for TO in the **D1–P3** duplex was much lower than in the single-stranded **P3**, a clear FRET from TO to Cy5 was observed (Fig. 2, red trace). Upon addition of fully complementary **D2**, the fluorescence intensity for both TO and Cy5 increased multiple times (Fig. 2, blue trace), signaling displacement of DNA strand **D1** from the TO-labeled PNA strand **P3**. As the displacement of **P3** from **D1** by **D2** leads to the hydrophobic ssPNA **P3**, we tentatively attribute the increase in Cy5 fluorescence to aggregation of the hydrophobic PNA **P3** to the Cy5 dye, which is also hydrophobic.

AFM analysis of the **D1–P3** duplex revealed dotted structures (see ESI, Fig. S9†), indicating formation of the expected circular DNA–PNA hybrid structures, and ruling out a considerable contribution from linear structures to the observed FRET signal in **D1–P3**. Since PNA-oligonucleotide hybrids usually offer higher stability towards enzymatic degradation,[7] this should allow utilization of our circular PNA–DNA/RNA complexes for cellular delivery based on our conjugation strategy.

Lastly, we studied the performance of a TO-labeled PNA, **P4**, in single nucleotide polymorphism (SNP) detection.[10a] We envisioned that our novel triazole-linked TO-PNA conjugate could, in principle, also be used for mismatch detection (Scheme 2b). We chose a reported DNA sequence **D6** (X = T) for which up to 3-fold match/mismatch discrimination using FIT-PNA at 25 °C was reported.[17] Upon hybridization of PNA **P4** to complementary **D6** (X = T) we observed a 5-fold enhancement of fluorescence (Fig. 3a). In comparison, changing the adjacent pyrimidine nucleobase into a mismatched pyrimidine (X = C, in **D7**) increased the fluorescence only 1.5-fold. Thus, we observed about 3.5-fold discrimination ability for the A–C match/mismatch pair, indicating good match/mismatch discrimination ability. Importantly, we observed a similar discriminating ability for other mismatches (X = G and A, **D8** and **D9**, respectively) as well, indicating the general applicability of our method (Fig. 3b).

In conclusion, we report a novel strategy for PNA functionalization that allows straightforward on-resin click modification. We demonstrate the applicability of the method by clicking TO at an internal position on the PNA. The azido- or TO-modified PNA is then hybridized to a fluorescent DNA strand to form a circular complex, allowing direct (*via* azido-

PNA
P3: Ac-Lys-taaagaaTOagacgcc-Lys-NH_2

DNA
D1: 5′-F-TTCTTTATGTTTTTGGCGTCT-Q-3′
D2: 5′-AGACGCCAAAAACATAAAGAA-3′

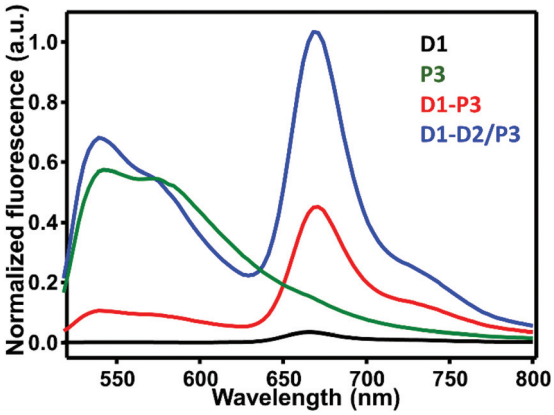

Fig. 2 Normalized fluorescence spectra showing the binding of antisense DNA **D1** to TO-labeled PNA **P3** (λ_{ex} = 510 nm).

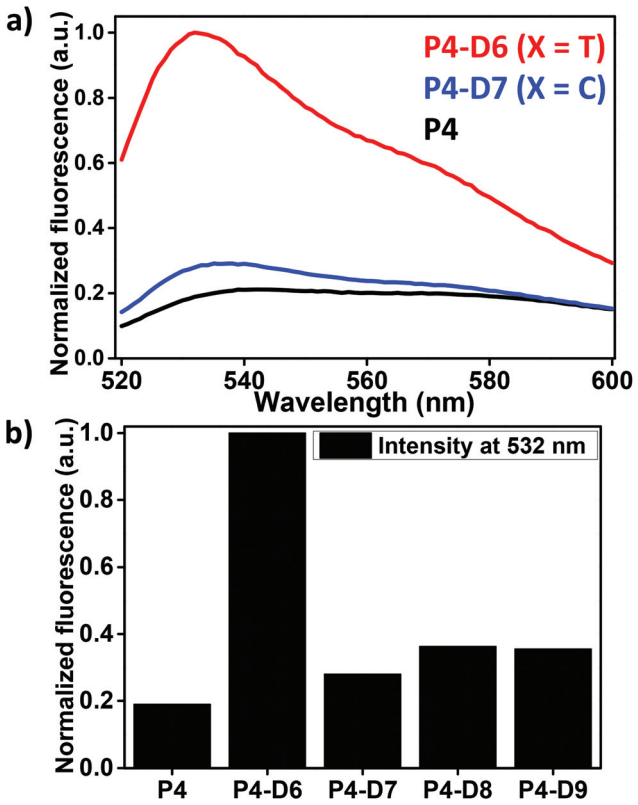

Fig. 3 (a) Normalized fluorescence spectra of PNA **P4** before and after addition of matched (**D6**) and mismatched (**D7**) DNA. (b) Normalized fluorescence showing the SNP-dependent decrease in fluorescence at 532 nm of **P4** with respect to all three mismatch base pairs next to the TO label. Measurement conditions: 1 μM PNA **P4** and DNA (**D6**–**D9**) in 10 mM NaH_2PO_4, 100 mM NaCl buffer at pH = 7.0, 25 °C, λ_{ex} = 510 nm.

PNA **P1**) and TO-assisted (*via* TO-PNA **P3**) sensing of the target DNA strand. In addition, we determined the SNP detection ability of a triazole linked dye on a FIT-PNA (**P4**) to be up to 3.5-fold match *vs.* mismatch. Since PNA–DNA hybrids generally show a higher stability towards exonuclease degradation, we believe that this work also provides a platform for different cellular delivery applications. Evaluation of PNA conjugates as a vector and protection agent for the delivery of an antisense sequence is ongoing.

We thank NanoNextNL (program 5A), a micro and nanotechnology consortium of the Government of The Netherlands and 130 partners for funding of this project. We also thank Dr Aart van Amerongen, Adrie Westphal, Antoine Moers, and Rickdeb Sen for fruitful discussions.

Notes and references

1 P. Nielsen, M. Egholm, R. Berg and O. Buchardt, *Science*, 1991, **254**, 1497.
2 H. Perry-O'Keefe, X.-W. Yao, J. M. Coull, M. Fuchs and M. Egholm, *Proc. Natl. Acad. Sci. U. S. A.*, 1996, **93**, 14670.
3 (*a*) H. J. Larsen, T. Bentin and P. E. Nielsen, *Biochim. Biophys. Acta*, 1999, **1489**, 159; (*b*) J. C. Hanvey, *et al.*, *Science*, 1992, **258**, 1481.
4 F. Hövelmann and O. Seitz, *Acc. Chem. Res.*, 2016, **49**, 714.
5 M. Egholm, O. Buchardt, P. E. Nielsen and R. H. Berg, *J. Am. Chem. Soc.*, 1992, **114**, 1895.
6 T. Vilaivan, *Acc. Chem. Res.*, 2015, **48**, 1645.
7 V. V. Demidov, V. N. Potaman, M. D. Frank–Kamenetskil, M. Egholm, O. Buchard, S. H. Sönnichsen and P. E. Nielsen, *Biochem. Pharmacol.*, 1994, **48**, 1310.
8 B. Hyrup and P. E. Nielsen, *Bioorg. Med. Chem.*, 1996, **4**, 5.
9 (*a*) P. E. Nielsen and T. Shiraishi, *Artif. DNA PNA XNA*, 2011, **2**, 90; (*b*) L. Fisher, U. Soomets, V. Cortes Toro, L. Chilton, Y. Jiang, U. Langel and K. Iverfeldt, *Gene Ther.*, 2004, **11**, 1264; (*c*) M. Kitamatsu, T. Kubo, R. Matsuzaki, T. Endoh, T. Ohtsuki and M. Sisido, *Bioorg. Med. Chem. Lett.*, 2009, **19**, 3410.
10 (*a*) M. Murtola and R. Strömberg, *Org. Biomol. Chem.*, 2008, **6**, 3837–3842; (*b*) M. Murtola, M. Wenska and R. Strömberg, *J. Am. Chem. Soc.*, 2010, **132**, 8984–8990; (*c*) A. Ghidini, M. Murtola and R. Strömberg, *Org. Biomol. Chem.*, 2016, **14**, 2768.
11 (*a*) O. Köhler and O. Seitz, *Chem. Commun.*, 2003, 2938; (*b*) O. Köhler, D. V. Jarikote and O. Seitz, *Chem. Commun.*, 2004, 2674; (*c*) O. Köhler, D. V. Jarikote and O. Seitz, *ChemBioChem*, 2005, **6**, 69.
12 E. Socher, D. V. Jarikote, A. Knoll, L. Röglin, J. Burmeister and O. Seitz, *Anal. Biochem.*, 2008, **375**, 318.
13 (*a*) K. Kaihatsu, D. A. Braasch, A. Cansizoglu and D. R. Corey, *Biochemistry*, 2002, **41**, 11118; (*b*) D. V. Jarikote, O. Köhler, E. Socher and O. Seitz, *Eur. J. Org. Chem.*, 2005, 3187; (*c*) B. Albada and N. Metzler-Nolte, *Chem. Rev.*, 2016, **116**, 11797.
14 W. Tang and M. L. Becker, *Chem. Soc. Rev.*, 2014, **43**, 7013.

15 A. Manicardi, A. Accetta, T. Tedeschi, S. Sforza, R. Marchelli and R. Corradini, *Artif. DNA PNA XNA*, 2012, **3**, 53.
16 (*a*) A. H. St. Amant, C. Engbers and R. H. E. Hudson, *Artif. DNA PNA XNA*, 2013, **4**, 4; (*b*) B. Ditmangklo, C. Boonlua, C. Suparpprom and T. Vilaivan, *Bioconjugate Chem.*, 2013, **24**, 614; (*c*) M. Strack, N. Metzler-Nolte and H. B. Albada, *Org. Lett.*, 2013, **15**, 3126; (*d*) M. Strack, S. Langklotz, J. E. Bandow, N. Metzler-Nolte and H. B. Albada, *J. Org. Chem.*, 2012, **77**, 9954.
17 D. G. Norman, R. J. Grainger, D. Uhrín and D. M. J. Lilley, *Biochemistry*, 2000, **39**, 6317.